Valence measurement of Mn oxides using Mn K_β emission spectroscopy

Q. Qian[a], T.A. Tyson[a], C.-C. Kao[b],*, J.-P. Rueff[b], F.M.F. deGroot[c], M. Croft[d],
S.-W. Cheong[d,e], M. Greenblatt[f], M.A. Subramanian[g]

[a]Department of Physics, New Jersey Institute of Technology, Newark, NJ 07102, USA
[b]Brookhaven National Laboratory, Upton, Long Island, NY 11973, USA
[c]Spectroscopy of Solids and Surfaces, University of Nijmegen, Toernooiveld, NL-6526 ED Nijmegen, Netherlands
[d]Department of Physics, Rutgers University, Piscataway, NJ 08855, USA
[e]Bell Laboratories, Lucent Technologies, Murray Hill, NJ 07974, USA
[f]Department of Chemistry, Rutgers University, Piscataway, NJ 08855, USA
[g]DuPont Central Research and Development, Wilmongton, DE 19880-0328, USA

Abstract

High resolution Mn K_β emission spectra provide a direct method to probe the effective spin state and charge density on Mn sites. Direct comparison of MnF_2 and MnO reveals significant changes due to the degree of covalency. The detailed shape and energy shift of the spectra for the perovskite $LaMnO_3$ and $CaMnO_3$ compounds are found to be very similar to Mn_2O_3 and MnO_2, respectively. Detailed Mn K_β X-ray emission results on $La_{1-x}Ca_xMnO_3$ can be well fit by linear superpositions of the end member spectra. However, for $x < 0.3$, a retarded response is found. No evidence for Mn^{2+} is found. © 2000 Elsevier Science Ltd. All rights reserved.

Keywords: Valence measurement

1. Introduction

The association of changes in resistivity with local structure in other oxide systems, such as the high temperature superconductors, strongly suggests the need for a systematic study of the local electronic and atomic structure in colossal magnetoresistance (CMR) systems. The class of $La_{1-x}A_xMnO_3$ (A = Ca, Sr, Ba, …) perovskite systems, are assumed to be mixed valent $[Mn^{3+}(d^4, t_{2g}^3 e_g^1)/Mn^{4+}(d^3, t_{2g}^3 e_g^0)]$, and exhibit a host of intriguing phenomena only on of which is CMR [1]. Experimentally, a direct coupling of the resistivity and bulk magnetization was found to exist [2]. It was observed by Asamitsu et al. [3], that the application of an external magnetic field induced a structural phase transition in $La_{0.83}Sr_{0.17}MnO_3$. For doping levels $x < 0.2$ and $x > 0.5$, the A = Ca system, for example, becomes an antiferromagnetic insulator [4]. Below the

insulator to metal transition temperature T_p, in the region $0.2 < x < 0.5$, these materials are ferromagnetic with conduction behavior characteristic of impure metals. Above this temperature (which is close to the ferromagnetic ordering temperature T_c), the resistivity curve bends over and displays semiconductor transport characterized by carriers excited across a narrow band gap.

In Zener's original double exchange model [5,6] for this system, the lattice is assumed to be rigid and ferromagnetism is induced by a spin coupling of the Mn^{4+} nearest-neighbor sites mediated by the e_g conduction electrons. Many recent experimental reports assume an ionic mixed-valence state of Mn in these materials—a central ingredient of double-exchange theory. However, there has been no systematic exploration of the exact valence and spin state of Mn in these systems. The purpose of this paper is to explore this area from the experimental perspective.

Measurements of the emission spectra have been complemented by detailed multiplet structure modeling [7]. Unlike
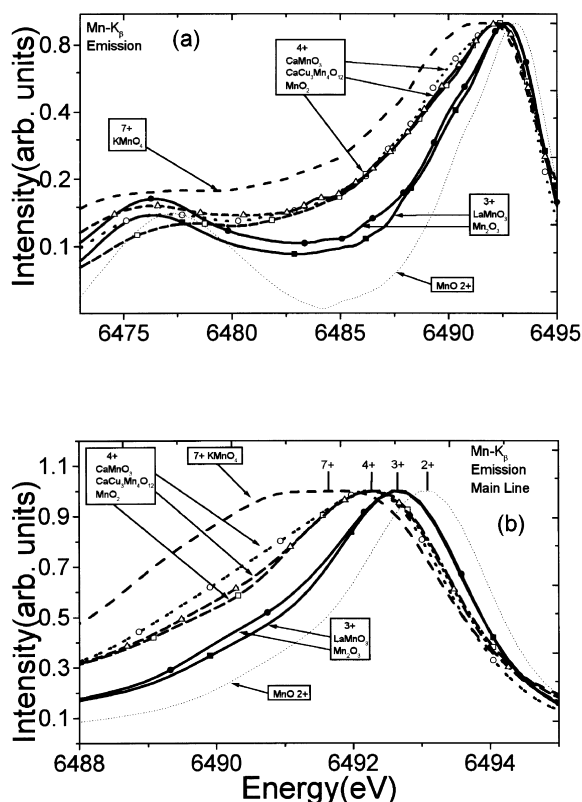
* Corresponding author.

Fig. 1. (a) MnK-edge X-ray emission spectra for model and end member compounds (log scale). Note that the spectra cluster according to oxidation state. The expanded main line spectra are shown in (b).
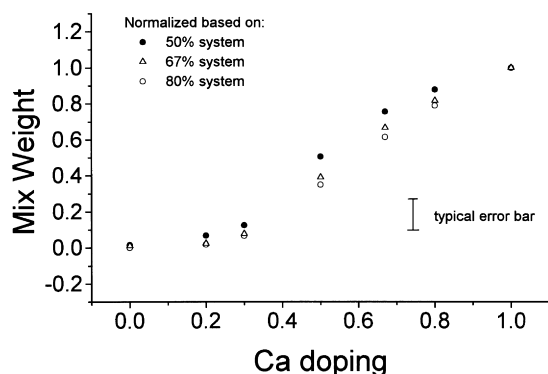

Fig. 2. Extracted coefficient x in the equation $x^* CaMnO_3 + (1 - x)^*$ $LaMnO_3$ as a function of the real Ca doping. Note the two-region doping behavior of the oxidation of the Mn sites as a function of Ca content. Points for end member normalization based on the 67 and 80% samples are also given. The shape of the curve is independent of the end member normalization procedure. The boundary between the regions seems to coincide with cross-over from ferromagnetic to antiferromagnetic behavior.

absorption edge measurements, the spectra yield information (main line positions and detail shapes) of the Mn sites which is not significantly affected by the geometry of the ligands. The changes in coordination and local structure, which accompany changes in valence, have less of an impact on emission measurements. Consequently, this approach is well suited to address the question of the nature of the valence of Mn in the CMR system.

2. Experimental and computational methods

Samples of $La_{1-x}Ca_xMnO_3$ series were synthesized and characterized as described in Ref. [8]. The $CaCu_3Mn_4O_{12}$ material was prepared as described in Refs. [9,10]. Fluorescence measurement samples were prepared by finely grinding the material and packing it onto adhesive tape. The Mn K_β fluorescence measurements were performed at the National Synchrotron Light Source's (NSLS) 27 pole wiggler Beamline X21A. The experimental set-up, which consists of an analyzer and detector in Rowland geometry, is described in Ref. [11]. Experimental and computational details can be found in Refs. [12,13]

3. Results, discussion and summary

Considering the multiple effects (spin coupling, crystal field splitting and exchange interactions) that combine to yield the Mn K_β emission spectrum energy position and structure, the utility of this spectroscopy for probing the Mn-valence state in a class of oxide materials will be addressed first. In Fig. 1(a), the Mn K_β spectra for a group of covalent Mn oxide compounds with varying formal valences are shown. A logarithmic intensity scale is used in this figure to aid in comparing the weak satellite region.

In Fig. 1(b), the vicinity of the main peak for these compounds is displayed on a linear scale. The MnO(2 +), $Mn_2O_3(3 +)$ and $MnO_2(4 +)$ binary standard compounds all have Mn in an octahedral environment while the $KMnO_4(+7)$ standard is tetrahedral. The perovskite $LaMnO_3(3 +)$ and $CaMnO_3(4 +)$ compounds, of course, also have octahedral Mn–O coordination. Finally, the quadrupled, distorted-perovskite $CaCu_3Mn_4O_{12}$ compound also has octahedral Mn coordination and has been recently shown to be a Mn(+4) compound [9,10].

Fig. 1(a) and (b) emphasizes that, for this rather broad group of materials, the spectra cluster into classes of curves which are determined by their valence. Specifically, the energy of main peak maximum, the spectral broadening on the high energy side of the main line, the depth of the spectral minimum between the main and satellite line, and the sharpness of the satellite line are all quite consistent for oxides in this group with the same formal Mn-valence. Thus, it is evident from Fig. 1a and b that (for such related oxides) different Mn-valence states produce distinct Mn K_β spectra and one can thereby make a Mn-valence state determination.
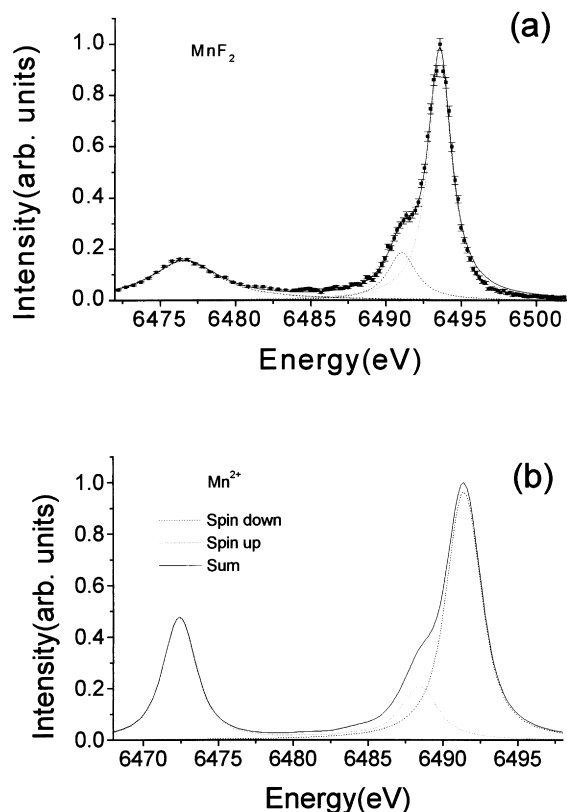
Fig. 3. Example of raw data, fits and simulations. (a) MnF_2 (Mn^{2+}) K_β spectrum with Lorentzian function fitting. Solid line is the sum of all components of fit. (b) The calculated MnK_β spectrum of Mn^{2+} ($10Dq = 1.5$ eV) showing the decomposition into mainly spin-up and spin-down 3p hole components relative to the 3d moment.

We performed measurements on the $La_{1-x}Ca_xMnO_3$ perovskites system with different Ca doping. Systematic shifts in peak positions are found by forming linear combinations of the end members. Although qualitative trends can be seen by looking at the raw spectra, a quantitative approach was found. First, the end member spectra (i.e. $x = 0$ and 1) were each fit to sum of four Voigt functions, the distribution of which were chosen both from the theoretical modeling and from the spectral shapes. The results of this fitting procedure for the end member perovskites is presented in Fig. 2. The fitted functional forms for the end members were then combined with the relative weights $w(x = 0)$ and $w(x = 1)$ (with $w(x = 0) + w(x = 1) = 1.0$) to model the intermediate-x spectra. The single weight parameter $w(x = 0)$ was then allowed to vary to give the best least squares fit to the intermediate spectra.

It is interesting to note that the fitted variation of $w(x = 0)$ is not simply equal to x as one would expect from a purely linear variation in the Mn-valence with x. Indeed, above $x \sim 0.3$ (Ca doping), one finds linear behavior with the expected slope while below $x \sim 0.3$, the slope is almost flat. The x-variation of the Mn K XAS chemical shift and pre-edge feature area (both indicators of Mn-valence variation) manifest a similar two-region behavior. Indeed, the effective unit cell volume also shows a similar behavior. These results again raise the question of whether there is an arrested Mn-3d hole variation, for low values of Ca substitution, in this system.

The method of fitting the Mn K_β emission spectra to a superposition of symmetrically peaked features has been applied to the other pure compound spectra considered here. The $2+$ Mn compound spectra were well fit by three features, as illustrated in Fig. 3(a) for the case of MnF_2. The comparison to the theoretical calculations for the Mn K_β emission spectrum (Fig. 3(b)) was performed using atomic multiplet plus an octahedral crystal field calculations for Mn^{2+} with $10Dq$ at 1.5 eV. The decomposition of the emission spectra into spin-up and spin-down components (relative to the 3d moment) was found and compared to experiments. A scaling factor of 80%, for the Slater integrals, was used in this calculation to account for covalency. (A similar scaling was used by Peng et al. [7] on Mn systems.)

Regarding the $La_{1-x}Ca_xMnO_3$ system, the Mn K_β emission results are consistent with a mixed valent Mn^{3+}/Mn^{4+} mixing that scales with the composition except for the $0 < x < 0.3$ range where the Mn-valence response appears arrested (with the apparent hole doping being nearly constant for $x < 0.3$). Indeed. the intermediate ($0.3 < x < 0.9$) spectra are well represented by linear superpositions of the $x = 0$ and $x = 1$ end point spectra in direct proportion to x. By contrast, this Mn K_β emission superposition method is inconsistent with Ca content below $x \sim 0.3$. This is the compositional range where the order switches from AF to FM and the origin of the arrested Mn-valence response at low x is potentially important. Finally, for the $La_{1-x}Ca_xMnO_3$ system, the Mn K_β emission results show absolutely no evidence for Mn^{2+} (which would have a quite distinct emission spectrum) and would appear to rule out the Mn^{2+}–Mn^{4+} disproportion mechanism. Interestingly, while Mn K XAS results evidence an average Mn-valence x-variation (for the $La_{1-x}Ca_xMnO_3$) which is similar to the Mn K_β emission results, the intermediate-x XAS spectra are far too sharp to be modeled by a superposition of the end point spectra [14]. Thus, the Mn K XAS (in this specific material at least) would appear to involve a time scale averaging that is longer than the emission spectroscopy.

References

[1] R. von Helmholt et al., J. Appl. Phys. 76 (1994) 6925 and references therein.
[2] M.F. Hundley et al., Appl. Phys. Lett. 67 (1995) 860.
[3] A. Asamitsu et al., Nature 373 (1995) 407.
[4] H.L. Lu et al., Appl. Phys. Lett. 65 (1994) 2108 and references therein.
[5] C. Zener, Phys. Rev. 81 (1951) 440.
[6] C. Zener, Phys. Rev. 82 (1951) 403.
[7] G. Peng et al., J. Am. Chem. Soc. 116 (1994) 2914.
[8] M. Croft et al., Phys. Rev. B 55 (1997) 8726.
[9] Z. Zeng et al., Phys. Rev. B 55 (1998) R595.
[10] Z. Zeng, M. Greenblatt, M.A. Subramanian, M. Croft, Phys. Rev. Lett. 82 (1999) 3164.
[11] C.-C. Kao et al., Rev. Sci. Inst. 66 (1995) 1699.
[12] T.A. Tyson et al., Phys. Rev. B 60 (1999) 4665.
[13] Q. Qian et al. in preparation.
[14] G. Subias et al., Phys. Rev. B 56 (1997) 8183.